

# Cs<sub>3</sub>Zn<sub>6</sub>B<sub>9</sub>O<sub>21</sub>: A Chemically Benign Member of the KBBF Family Exhibiting the Largest Second Harmonic Generation Response

Hongwei Yu,<sup>†,‡</sup> Hongping Wu,<sup>†</sup> Shilie Pan,<sup>†,\*</sup> Zhihua Yang,<sup>†</sup> Xueling Hou,<sup>†</sup> Xin Su,<sup>†</sup> Qun Jing,<sup>†,‡</sup> Kenneth R. Poeppelmeier,<sup>§,\*</sup> and James M. Rondinelli<sup>||,\*</sup>

<sup>†</sup>Key Laboratory of Functional Materials and Devices for Special Environments of CAS; Xinjiang Technical Institute of Physics & Chemistry of CAS; Xinjiang Key Laboratory of Electronic Information Materials and Devices, 40-1 South Beijing Road, Urumqi 830011, China

<sup>‡</sup>University of Chinese Academy of Sciences, Beijing 100049, China

<sup>§</sup>Department of Chemistry, Northwestern University, 2145 Sheridan Road, Evanston, Illinois 60208-3113, United States

<sup>||</sup>Department of Materials Science and Engineering, Drexel University, Philadelphia, Pennsylvania 19104-2816, United States

## Supporting Information

**ABSTRACT:** Nonlinear optical (NLO) crystals are essential materials for generation of coherent UV light in solid state lasers. KBBF is the only material that can achieve coherent light below 200 nm by direct second harmonic generation (SHG). However, its strong layer habits and the high toxicity of the beryllium oxide powders required for synthesis limit its application. By substituting Be with Zn and connecting adjacent [Zn<sub>2</sub>BO<sub>3</sub>O<sub>2</sub>]<sub>∞</sub> layers by B<sub>3</sub>O<sub>6</sub> groups, a new UV nonlinear optical material, Cs<sub>3</sub>Zn<sub>6</sub>B<sub>9</sub>O<sub>21</sub>, was synthesized. It overcomes the processing limitations of KBBF and exhibits the largest SHG response in the KBBF family.

Nonlinear optical (NLO) crystals, which are key materials for solid state lasers to produce coherent light through cascaded frequency conversion, have attracted considerable attention.<sup>1–8</sup> Many efforts have been made to understand the relationship among the composition, structure, and NLO properties of crystals; however, it remains challenging to efficiently design a suitable high-performing NLO material. A successful example is KBBF,<sup>1d,9</sup> which possesses moderate second harmonic generation (SHG) coefficients and large birefringence. It is the only material that can generate coherent light at wavelengths below 200 nm by direct SHG response. The excellent properties of KBBF arise mainly from the [Be<sub>2</sub>BO<sub>3</sub>F<sub>2</sub>]<sub>∞</sub> layers in its chiral structure,<sup>9</sup> which contain BO<sub>3</sub> groups that adopt a coplanar configuration promoting birefringence and SHG. The three terminal oxygen atoms of the BO<sub>3</sub> group are linked with Be atoms, eliminating three dangling bonds of the BO<sub>3</sub> groups, which further widens its transparency in the UV region. However, the weak K<sup>+</sup>–F<sup>–</sup> ionic interactions between adjacent [Be<sub>2</sub>BO<sub>3</sub>F<sub>2</sub>]<sub>∞</sub> layers make KBBF exhibit a strong layer habit, which limits its applications owing to difficulties in processing.

In a search to overcome the layer habit, the Sr<sub>2</sub>Be<sub>2</sub>B<sub>2</sub>O<sub>7</sub> (SBBO) family of crystals were found by Chen, et al.<sup>10–13</sup> The basic structure unit in the SBBO family is a [M<sub>2</sub>(BO<sub>3</sub>)<sub>2</sub>O]<sub>∞</sub> (M = Be or Al) double layer, which makes them easier to grow in larger sizes. The SBBO family also generally exhibits a larger

SHG response than KBBF owing to the higher number density of BO<sub>3</sub> triangles in the [M<sub>2</sub>(BO<sub>3</sub>)<sub>2</sub>O]<sub>∞</sub> double layer.<sup>10</sup> However, these layers are separated by either alkaline or alkaline earth cations, which practically leads to polydomain crystals during growth. Such domain structures lead to undesirable optical nonuniformity in the SBBO family.<sup>14</sup> In 2010 and 2011, Ye, et al. reported a series of alkaline beryllium borates.<sup>15,16</sup> In the beryllium borates, the [Be<sub>2</sub>BO<sub>3</sub>F<sub>2</sub>]<sub>∞</sub> layers found in KBBF are fully oxygenated into [Be<sub>2</sub>BO<sub>3</sub>O<sub>2</sub>]<sub>∞</sub> sheets, and adjacent [Be<sub>2</sub>BO<sub>3</sub>O<sub>2</sub>]<sub>∞</sub> layers are bridged by B–O groups, which mitigate the strong layer habit of KBBF. Because of the high toxicity of the beryllium oxide powders, however, it remains challenging to safely grow crystals of large size.

Recognizing that Zn atoms are generally coordinated by four O atoms (tetrahedral) and the Zn–O bond length is also close to that of Be–O, we sought to link the coplanar BO<sub>3</sub> triangles with ZnO<sub>4</sub> tetrahedra, forming [Be<sub>2</sub>BO<sub>3</sub>O<sub>2</sub>]<sub>∞</sub>-like layers, which partly maintains the optical properties of KBBF yet overcome its strong layer topology during growth. Moreover, substitution of Zn for Be eliminates the toxicity issues inherent in synthesis of KBBF and SBBO from beryllium oxide powders. In addition, the distorted ZnO<sub>4</sub> tetrahedra should provide an enhanced contribution to the SHG response.<sup>17</sup> Guided by these ideas, a new NLO crystal, Cs<sub>3</sub>Zn<sub>6</sub>B<sub>9</sub>O<sub>21</sub> (CZB), was synthesized. Its crystal structure consists of the targeted [Zn<sub>2</sub>BO<sub>3</sub>O<sub>2</sub>]<sub>∞</sub> layers with adjacent layers connected by B<sub>3</sub>O<sub>6</sub> groups. Remarkably it exhibits the largest SHG response in the KBBF family, approximately 3.3 times that of KDP despite a reduced BO<sub>3</sub> number density.

CZB crystallizes in space group *Cmc*2<sub>1</sub> (no. 36) of the orthorhombic system. In the asymmetric unit, there are 3 unique Cs atoms, 3 unique Zn atoms, 6 unique B atoms, and 12 unique O atoms (Table S2 in the Supporting Information (SI)). The crystal structure of CZB is depicted in Figure 1. All B atoms are coordinated to three O atoms to form planar BO<sub>3</sub> triangles. Interestingly, B(3)O<sub>3</sub>, B(4)O<sub>3</sub>, and B(5)O<sub>3</sub> triangles connect with each other to form the B<sub>3</sub>O<sub>6</sub> groups, while the B(1)O<sub>3</sub>, B(2)O<sub>3</sub>, and B(6)O<sub>3</sub> are the isolated triangles. The

Received: November 18, 2013

Published: January 6, 2014

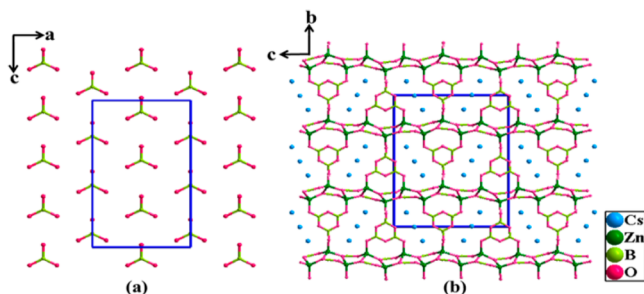


**Figure 1.** (a) The nearly coplanar  $\text{BO}_3$  triangles in CZB. (b) The 3D network of CZB view down the  $a$  axis.

different constituent B–O groups present in CZB do not follow the fifth rule of Pauling, which states that identical repeating chemical groups are expected because each atom is most stable in a specific environment. In CZB the isolated triangles adopt a nearly coplanar configuration (Figure 1a), which is established to be favorable for generating large SHG responses and birefringence in borates. Further, the coplanar  $\text{BO}_3$  triangles are connected by  $\text{ZnO}_4$  tetrahedra to form two-dimensional (2D)  $[\text{Zn}_2\text{BO}_3\text{O}_2]_\infty$  layers extending in the (010) plane, which are linked by the  $\text{B}_3\text{O}_6$  groups with alternating orientation, forming a 3D  $[\text{Zn}_2\text{B}_3\text{O}_7]_\infty$  framework. The Cs atoms fill the space provided by the  $[\text{Zn}_2\text{B}_3\text{O}_7]_\infty$  framework to balance charge (Figure 1b) and possess two different coordination environments. The Cs(1) and Cs(3) atoms are coordinated by eight O atoms, and the Cs(2) atom is coordinated by seven O atoms, with the Cs–O bond lengths varying from 3.147(5) to 3.430(3) Å. The Zn atoms are bound to four O atoms to form distorted  $\text{ZnO}_4$  tetrahedra with Zn–O bond lengths ranging from 1.902(2) to 1.982(3) Å. All B atoms are coordinated to three O atoms to form  $\text{BO}_3$  triangles with the B–O bond lengths ranging from 1.284(16) to 1.407(17) Å. All of the bond lengths are consistent with those in other compounds,<sup>18</sup> and the IR spectrum (Figure S3 in the SI) and the bond valence sums of each atom<sup>19,20</sup> (Table S2 in the SI) also justify the assigned coordination environments.

CZB contains interesting  $[\text{Zn}_2\text{BO}_3\text{O}_2]_\infty$  layers, which are similar to the  $[\text{Be}_2\text{BO}_3\text{F}_2]_\infty$  layer in KBBF, making it a new member in the family. It is worth noting that the adjacent  $[\text{Zn}_2\text{BO}_3\text{O}_2]_\infty$  layers in CZB, however, are connected by the  $\text{B}_3\text{O}_6$  planar groups, which suggests CZB will grow without layer habits (Figure S2 in the SI). The DSC curve shows two endothermic peaks, and there is obvious weight loss on the TG curve along with the first endothermic peak (Figure S5 in the SI), suggesting that CZB melts incongruently. The residue in the platinum pan after TG/DSC measurement was proved to be  $\text{Zn}_3(\text{BO}_3)_2$  by powder X-ray diffraction (Figure S6 in the SI).

It is widely considered that the excellent linear and nonlinear optical properties of KBBF-structured materials originate from the  $[\text{M}_2\text{BO}_3\text{X}_2]_\infty$  layer ( $\text{M}$  = divalent metal cation,  $\text{X}$  = F, O);<sup>1d,9,14–16</sup> thus, good NLO properties in CZB are also expected. The optical diffuse reflectance spectrum of CZB was measured (Figure S4 in the SI). It is clear that there is no absorption peaks from 360 to 2600 nm and the cutoff edge is near 200 nm. The wide transparency window will be favorable for the application of CZB in the UV. The plot of the second-harmonic intensity vs particle size of the CZB powders is shown in Figure 2. The results are consistent with phase-matching behavior according to the rule proposed by Kurtz and

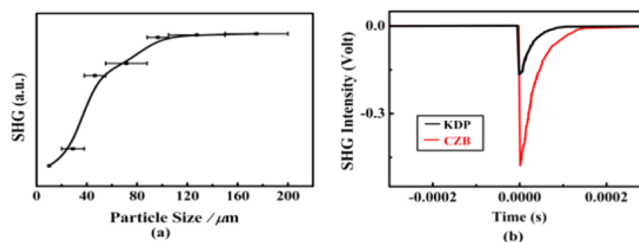


**Figure 2.** (a) Phase-matching curve for CZB. (The solid curve drawn is to guide the eye and is not a fit to the data.) (b) SHG intensities of CZB with commercial KDP as a reference: Oscilloscope traces from the same particle size (88–105  $\mu\text{m}$ ) of powder of KDP and CZB. At 88–105  $\mu\text{m}$ , the SHG intensity of CZB is saturated.

Perry.<sup>21</sup> The SHG measurements on a Q-switched Nd:YAG laser with the sieved powder sample revealed that the SHG signal of CZB is about 3.3 times that of KDP, the largest SHG response in the KBBF family, including  $\text{M}'\text{Be}_2\text{BO}_3\text{F}_2$  ( $\text{M}'$  = K, Rb, Cs),  $\beta\text{-KBe}_2\text{B}_3\text{O}_7$ ,  $\text{RbBe}_2\text{B}_3\text{O}_7$ ,  $\gamma\text{-KBe}_2\text{B}_3\text{O}_7$ , and  $\text{Na}_2\text{CsBe}_6\text{B}_3\text{O}_{15}$ .

According to the anionic group theory, the SHG responses in the borates mainly originate from the B–O groups. For the KBBF derivatives, they may contain two types of B–O groups. One group consists of the coparallel  $\text{BO}_3$  triangles. The other group, located between and connecting the two adjacent  $[\text{Be}_2\text{BO}_3\text{O}_2]$  together, often possesses an antiparallel arrangement, which would cancel any contribution to the macroscopic SHG response. Therefore, the SHG responses of the KBBF derivatives will mainly arise from the coparallel  $\text{BO}_3$  triangles. Specifically, the number density of the coparallel  $\text{BO}_3$  triangles will determine the SHG responses of the KBBF family of compounds.<sup>10,12</sup>

For CZB, the  $\text{B}_3\text{O}_6$  groups are found between adjacent  $[\text{Zn}_2\text{BO}_3\text{O}_2]$  layers and are antialigned (Figure 1b). So it seems that the SHG response of CZB should also come from the coparallel  $\text{BO}_3$  triangles. However, it is difficult to understand the large SHG response of CZB by only considering the number density of the  $\text{BO}_3$  triangles, because CZB has the *smallest* density of the  $\text{BO}_3$  triangles yet exhibits the *largest* SHG response in the KBBF family (Table 1). It is worth noting that

**Table 1. Structure–NLO Property Comparison for Compounds in the KBBF Family**

| compounds  | space group | SHG response (KDP) | $\text{BO}_3$ number density ( $\times 10^{-3}$ ) |
|--|-------------|--------------------|---|
| $\text{M}'\text{Be}_2\text{BO}_3\text{F}_2$ <sup>2,16</sup> ( $\text{M}'$ = K, Rb, Cs) | R32         | 0.95–1.26          | 8.32–9.46   |
| $\beta\text{-KBe}_2\text{B}_3\text{O}_7$ <sup>15</sup>                                 | $Pmn2_1$    | 0.75               | 6.85  |
| $\gamma\text{-KBe}_2\text{B}_3\text{O}_7$ <sup>15</sup>                                | $P2_1$      | 0.68               | 6.96  |
| $\text{RbBe}_2\text{B}_3\text{O}_7$ <sup>15</sup>                                      | $Pmn2_1$    | 0.79               | 6.68  |
| $\text{Na}_2\text{CsBe}_6\text{B}_3\text{O}_{15}$ <sup>16</sup>                        | C2          | 1.17               | 9.21  |
| CZB  | $Cmc2_1$    | 3.30               | 5.09  |

the  $\text{ZnO}_4$  tetrahedra with  $d^{10}$   $\text{Zn}^{2+}$  cations may also be NLO-active groups. Therefore, to better understand the contributions to the SHG from these NLO-active groups in CZB, we quantified each unit's dipole moment in the unit cell with a simple bond-valence approach (Table 2).<sup>22</sup> It is clear that the  $\text{B}_3\text{O}_6$  groups,  $\text{BO}_3$  triangles, and  $\text{ZnO}_4$  tetrahedra yield dipole moments of 0.27, 5.53, and 12.53 D in the unit cell, respectively. The net dipole moment of the  $\text{BO}_3$  triangles and  $\text{ZnO}_4$  tetrahedra both are directed along the polar  $c$ -axis,

**Table 2. Direction and Magnitude of the Dipole Moments in the BO<sub>3</sub> Triangles and ZnO<sub>4</sub> Tetrahedra and Their Contributions to the Polarization in the Unit Cell**

| species                            | $x(a)$ | $y(b)$ | $z(c)$ | magnitude |                                 |
|------------------------------------|--------|--------|--------|-----------|---------------------------------|
|                                    |        |        |        | debye     | $10^{-4}$ esu-cm/Å <sup>3</sup> |
| B(1)O <sub>3</sub>                 | 0      | 0.32   | -0.56  | 0.64      | 10.85                           |
| B(2)O <sub>3</sub>                 | 0      | 0.65   | -0.15  | 0.66      | 11.24                           |
| B(6)O <sub>3</sub>                 | 0      | -0.07  | -0.22  | 0.23      | 3.83                            |
| B <sub>3</sub> O <sub>6</sub>      | 0.17   | -0.37  | -0.04  | 0.40      | 6.90                            |
| Zn(1)O <sub>4</sub>                | -1.17  | 0.32   | -0.43  | 1.29      | 21.87                           |
| Zn(2)O <sub>4</sub>                | 0.43   | 1.33   | 0.20   | 1.41      | 23.94                           |
| Zn(3)O <sub>4</sub>                | -0.55  | -1.00  | -1.33  | 1.75      | 29.73                           |
| BO <sub>3</sub>                    | 0      | 0      | -5.53  | -         | 24.63                           |
| unit B <sub>3</sub> O <sub>6</sub> | 0      | 0      | -0.27  | -         | 1.15                            |
| cell ZnO <sub>4</sub>              | 0      | 0      | -12.53 | -         | 53.17                           |
| total                              | 0      | 0      | -18.33 | -         | 77.79                           |

which indicates that the SHG response of CZB arises from both the BO<sub>3</sub> triangles and ZnO<sub>4</sub> tetrahedra, while the B<sub>3</sub>O<sub>6</sub> groups contribute little.

We explore the additive effect of the polar distortions by including the full symmetry of the crystal by using a mode-polarization vector analysis.<sup>23,24</sup> In this way, we rigorously isolate the atomic contribution to inversion symmetry breaking in CZB. We quantify the distortions using the orthonormal symmetry-adapted basis set of a pseudosymmetric *Cmcm* structure. Structural details are given in Table S4 in the SI. The polar *Cmc*<sub>2</sub> structure is related to the *Cmcm* phase via a single displacive mode transforming as the irreducible representation  $\Gamma_2^-$ . It involves displacements of all the atoms except Cs, largely along the crystallographic (polar) *c* axis (Figure 3). The Zn atoms only make small displacements within the ZnO<sub>4</sub> polyhedra relative to the centrosymmetric reference structure (Figure 3a). The loss of inversion symmetry is largely mediated by displacements of the oxygen atoms of the ZnO<sub>4</sub> tetrahedra and the BO<sub>3</sub> rings along the polar *c* axis (Figure 3b). Each of the triangular arrays displace in the same direction, with chains of disconnected BO<sub>3</sub> units separating the triangular arrays displacing in the opposite direction, leading to a partial cancellation of the electric dipole in the unit cell (Figure 3c).

Next, the total mode-distortion vector amplitude is computed following the procedure described in ref 23. We find a value of 4.56 Å, which should be compared to 1.46 Å computed for KBBF (see SI), i.e., approximately 3 × larger. This additional amount of polar displacements in CZB compared to KBBF can be attributed to both the distorted ZnO<sub>4</sub> tetrahedra and importantly the *distorted* BO<sub>3</sub> rings in

CZB. Boron does not sit in the center of the triangular units, whereas it does in KBBF, a crucial difference. Besides KBBF being chiral, its BO<sub>3</sub> rings are regular with 120° B–O–B angles. Thus, a subtle balance between polar displacements arising from the two structural motifs must be considered when explaining the enhanced SHG of CZB. The largest SHG response in the KBBF-structure family is observed in CZB because of both acentric BO<sub>3</sub> triangles, despite a smaller number density of them, and distorted ZnO<sub>4</sub> tetrahedra.

To explore the intrinsic relationship between the electronic structure and optical properties, electronic band structures are also calculated using CASTEP (Figure S7 in the SI). CZB is found to be an indirect gap crystal (3.45 eV) with a valence band (VB) maximum at the Y point and a conduction band (CB) minimum at the  $\Gamma$ -point (Figure S7a in the SI). The upper region of the VB is mainly derived from O 2*p* and Zn 3*d* orbitals with a tiny contribution of Cs 5*p* and B 2*p* states, and the bottom of the CB is mainly composed of O 2*p*, B 2*p* and Zn 3*s* states mixing with a small amount of Cs 5*p* states (Figure S7b in the SI). The linear and nonlinear optical properties are directly related to the electronic transitions between the energy levels close to the forbidden band,<sup>25</sup> which further supports the concept that both the BO<sub>3</sub> triangles and ZnO<sub>4</sub> tetrahedra contribute to the SHG.

On the basis of the dielectric function  $\epsilon(\omega) = \epsilon_1(\omega) + i\epsilon_2(\omega)$ , the linear optical properties were also examined. The imaginary part  $\epsilon_2$  is calculated in CASTEP numerically by evaluating all the transitions from occupied to unoccupied states in the Brillouin zone. A Kramers–Kronig transformation<sup>26</sup> provides the real part  $\epsilon_1$  of the dielectric function. Further, the refractive indices  $n(\omega)$  and birefringence ( $\Delta n$ ) are also calculated, the latter shown in Figure S9 in the SI. It is clear that CZB possesses a moderate birefringence with  $\Delta n = 0.062$  at 532 nm.

The SHG coefficients were obtained with ab initio electronic structure calculations. CZB exhibits *mm*2 point symmetry; consequently, it has three independent second-order dielectric tensor elements under the restriction of Kleinman symmetry which are related to the  $d_{31}$ ,  $d_{32}$ , and  $d_{33}$  SHG coefficients. For CZB, we find  $d_{31} = 1.06$  pm/V,  $d_{32} = -0.08$  pm/V,  $d_{33} = -1.03$  pm/V, respectively. Among them,  $d_{31}$  and  $d_{33}$  are approximately three times that of KDP, which is consistent with the experimental results.

In conclusion, the substitution of Zn for Be atom generates a KBBF-type structure, Cs<sub>3</sub>Zn<sub>6</sub>B<sub>9</sub>O<sub>21</sub>. It overcomes the layer habits of KBBF and exhibits a SHG response about 3.3 times that of KDP, which is largest in the KBBF family. The calculations of the dipole moments, identification of the inversion symmetry lifting atomic distortions, and electronic

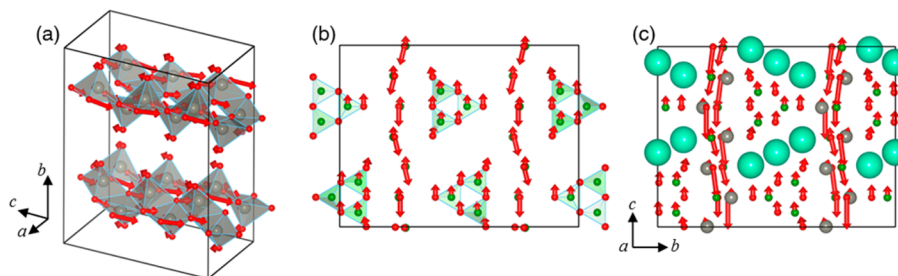


**Figure 3.** Atomic distortion patterns obtained from the symmetry-mode analysis: Oxygen atom displacements belonging to (a) the ZnO<sub>4</sub> tetrahedra, (b) the BO<sub>3</sub> network, and (c) the complete distortion projected along the *a* axis.



structure reveal that the enhanced SHG response originates from the cooperative effect of coparallel  $\text{BO}_3$  triangles and distorted  $\text{ZnO}_4$  tetrahedra in the  $[\text{Zn}_2\text{BO}_3\text{O}_2]_\infty$  layers. We conjecture that using Zn atoms to substitute for Be in known beryllium borates is a promising method to achieve facile synthesis of useful NLO crystals while also increasing the SHG response. Similar substitution attempts in other beryllium borates are in progress.

## ■ ASSOCIATED CONTENT

### ■ Supporting Information

Crystallographic data (CIF), experimental and theoretical methods, and additional tables and figures. This material is available free of charge via the Internet at <http://pubs.acs.org>.

## ■ AUTHOR INFORMATION

### Corresponding Author

s1pan@ms.xjb.ac.cn; jrondinelli@coe.drexel.edu; krp@northwestern.edu

### Notes

The authors declare no competing financial interest.

## ■ ACKNOWLEDGMENTS

This work is supported by 973 Program of China (Grant No. 2012CB626803), the High Technology Research & Development Program of Xinjiang Uygur Autonomous Region of China (Grant No. 201315103, 201116143), the National Natural Science Foundation of China (Grant Nos. U1129301, 21201176, 51172277), the Western Light Foundation Program of CAS (Grant No. XBBS201214), Main Direction Program of Knowledge Innovation of CAS (Grant No. KJJCX2-EW-H03-03). K.R.P. acknowledges support from the National Science Foundation (Solid State Chemistry Award No. DMR-1005827); J.M.R. acknowledges support from ACS PRF (52138-DNI10).

## ■ REFERENCES

- (1) (a) Chen, C. T.; Wu, B. C.; Jiang, A. D.; You, G. M. *Sci. Sin., Ser. B (Engl. Ed.)* **1985**, *28*, 235. (b) Chen, C. T.; Wu, Y. C.; Jiang, A. D.; You, G. M.; Li, R. K.; Lin, S. J. *J. Opt. Soc. Am. B* **1989**, *6*, 616. (c) Wu, Y. C.; Sasaki, T.; Nakai, S.; Yokotani, A.; Tang, H.; Chen, C. T. *Appl. Phys. Lett.* **1993**, *62*, 2614. (d) Chen, C. T.; Lu, J. H.; Togashi, T.; Suganuma, T.; Sekikawa, T.; Watanabe, S.; Xu, Z. Y.; Wang, J. Y. *Opt. Lett.* **2002**, *27*, 637. (e) Yap, Y. K.; Inagaki, M.; Nakajima, S.; Mori, Y.; Sasaki, T. *Opt. Lett.* **1996**, *21*, 1348.
- (2) (a) Mei, L.; Huang, X.; Wang, Y.; Wu, Q.; Wu, B.; Chen, C. Z. *Kristallogr.* **1995**, *210*, 93. (b) Chen, C. T.; Luo, S. Y.; Wang, X. Y.; Wang, G. L.; Wen, X. H.; Wu, H. X.; Zhang, X.; Xu, Z. Y. *J. Opt. Soc. Am. B* **2009**, *26*, 1519. (c) Huang, H. W.; Chen, C. T.; Wang, X. Y.; Zhu, Y.; Wang, G. L.; Zhang, X.; Wang, L. R.; Yao, J. Y. *J. Opt. Soc. Am. B* **2011**, *28*, 2186.
- (3) (a) Maggard, P. A.; Stern, C. L.; Poeppelmeier, K. R. *J. Am. Chem. Soc.* **2001**, *123*, 7742. (b) Pan, S. L.; Smit, J. P.; Watkins, B.; Marvel, M. R.; Stern, C. L.; Poeppelmeier, K. R. *J. Am. Chem. Soc.* **2006**, *128*, 11631. (c) Halasyamani, P. S.; Poeppelmeier, K. R. *Chem. Mater.* **1998**, *10*, 2753.
- (4) (a) Wu, H. P.; Pan, S. L.; Poeppelmeier, K. R.; Li, H. Y.; Jia, D. Z.; Chen, Z. H.; Fan, X. Y.; Yang, Y.; Rondinelli, J. M.; Luo, H. *J. Am. Chem. Soc.* **2011**, *133*, 7786. (b) Yu, H. W.; Pan, S. L.; Wu, H. P.; Zhao, W. W.; Zhang, F. F.; Li, H. Y.; Yang, Z. H. *J. Mater. Chem.* **2012**, *22*, 2105. (c) Yu, H. W.; Wu, H. P.; Pan, S. L.; Yang, Z. H.; Su, X.; Zhang, F. F. *J. Mater. Chem.* **2012**, *22*, 9665.
- (5) (a) Halasyamani, P. S.; O'Hare, D. *Chem. Mater.* **1998**, *10*, 646. (b) Turp, S. A.; Hargreaves, J.; Baek, J.; Halasyamani, P. S.; Hayward, M. A. *Chem. Mater.* **2010**, *22*, 5580. (c) Sun, C. F.; Hu, C. L.; Xu, X.;

Yang, B. P.; Mao, J. G. *J. Am. Chem. Soc.* **2011**, *133*, 5561. (d) Yang, B. P.; Hu, C. L.; Xu, X.; Sun, C. F.; Zhang, J. H.; Mao, J. G. *Chem. Mater.* **2010**, *22*, 1545.

(6) (a) Yuan, G.; Xue, D. *Acta Crystallogr., Sect. B: Struct. Sci.* **2007**, *63*, 353. (b) Xue, D.; Betzler, K.; Hesse, H. *Appl. Phys. A: Mater. Sci. Process.* **2002**, *74*, 779.

(7) (a) Hu, Z. G.; Yoshimura, M.; Muramatsu, K.; Mori, Y.; Sasaki, T. *J. Appl. Phys.* **2002**, *41*, 1131. (b) Schaffers, K. L.; Deloach, L. D.; Payne, S. A. *IEEE J. Quantum Electron.* **1996**, *32*, 741. (c) Paul, A. K.; Sachidananda, K.; Natarajan, S. *Cryst. Growth Des.* **2010**, *10*, 456.

(8) (a) Keszler, D. A. *Curr. Opin. Solid State Mater. Sci.* **1996**, *1*, 204. (b) Zhang, W. L.; Cheng, W. D.; Zhang, H.; Geng, L.; Lin, C. S.; He, Z. Z. *J. Am. Chem. Soc.* **2010**, *132*, 1508.

(9) (a) Wu, B. C.; Tang, D. Y.; Ye, N.; Chen, C. T. *Opt. Mater.* **1996**, *5*, 105. (b) Chen, C. T.; Wang, G. L.; Wang, X. Y.; Xu, Z. Y. *Appl. Phys. B: Lasers Opt.* **2009**, *97*, 9.

(10) Chen, C. T.; Wang, Y. B.; Wu, B. C.; Wu, K.; Zeng, W.; Yu, L. H. *Nature* **1995**, *373*, 322.

(11) Qi, H.; Chen, C. T. *Chem. Lett.* **2001**, *30*, 354.

(12) Ye, N.; Zeng, W. R.; Wu, B. C.; Huang, X. Y.; Chen, C. T. *Z. Kristallogr.* **1998**, *213*, 452.

(13) Ye, N.; Zeng, W. R.; Jiang, J.; Wu, B. C.; Chen, C. T.; Feng, B. H.; Zhang, X. L. *J. Opt. Soc. Am. B* **2000**, *17*, 764.

(14) Chen, C. T.; Bai, L.; Wang, Z. Z.; Li, R. K. *J. Cryst. Growth* **2006**, *292*, 169.

(15) Wang, S. C.; Ye, N. *J. Am. Chem. Soc.* **2011**, *133*, 11458.

(16) Wang, S. C.; Ye, N.; Li, W.; Zhao, D. *J. Am. Chem. Soc.* **2010**, *132*, 8779.

(17) (a) Inaguma, Y.; Yoshida, M.; Katsumata, T. *J. Am. Chem. Soc.* **2008**, *130*, 6704. (b) Li, F.; Pan, S. L.; Hou, X. L.; Yao, J. Y. *Cryst. Growth Des.* **2009**, *9*, 4091.

(18) (a) Huang, Z. J.; Pan, S. L.; Yang, Z. H.; Yu, H. W.; Dong, X. Y.; Zhao, W. W.; Dong, L. Y.; Su, X. *Solid State Sci.* **2013**, *15*, 73. (b) Yu, H. W.; Wu, H. P.; Pan, S. L.; Zhang, B. B.; Wen, M.; Yang, Z. H.; Li, H. Y.; Jiang, X. Z. *Eur. J. Inorg. Chem.* **2013**, *2013*, 5528.

(19) Brese, N. E.; O'Keeffe, M. *Acta Crystallogr., Sect. B: Struct. Sci.* **1991**, *47*, 192.

(20) Brown, I. D.; Altermatt, D. *Acta Crystallogr., Sect. B: Struct. Sci.* **1985**, *41*, 244.

(21) Kurtz, S. K.; Perry, T. T. *J. Appl. Phys.* **1968**, *39*, 3798.

(22) (a) Kim, J. H.; Halasyamani, P. S. *J. Solid State Chem.* **2008**, *181*, 2108. (b) Ok, K. M.; Halasyamani, P. S. *Inorg. Chem.* **2005**, *44*, 3919. (c) Izumi, H. K.; Kirsch, J. E.; Stern, C. L.; Poeppelmeier, K. R. *Inorg. Chem.* **2005**, *44*, 884. (d) Maggard, P. A.; Nault, T. S.; Stern, C. L.; Poeppelmeier, K. R. *J. Solid State Chem.* **2003**, *175*, 27.

(23) Wu, H. P.; Yu, H. W.; Yang, Z. H.; Hou, X. L.; Su, X.; Pan, S. L.; Poeppelmeier, K. R.; Rondinelli, J. M. *J. Am. Chem. Soc.* **2013**, *135*, 4215.

(24) Perez-Mato, J. M.; Orobengoa, D.; Aroyo, M. I. *Acta Crystallogr., Sect. A: Found. Crystallogr.* **2010**, *66*, 558.

(25) Zhao, S.; Jiang, X.; He, R.; Zhang, S. Q.; Sun, Z.; Luo, J.; Lin, Z.; Hong, M. C. *J. Mater. Chem. C* **2013**, *1*, 2906.

(26) Wooten, F. *Optical Properties of Solid*; Academic: New York, 1972.